



# Moisture sorption isotherms and thermodynamic properties of sorbed water of chironji (*Buchanania lanzan* Spreng.) kernels at different storage conditions

S. N. Sahu<sup>1,2,3</sup> · Anupam Tiwari<sup>1</sup> · J. K. Sahu<sup>1</sup> · S. N. Naik<sup>1</sup> · I. Baitharu<sup>2,3</sup> · E. Kariali<sup>2,3</sup>

Received: 30 May 2018 / Accepted: 10 July 2018 / Published online: 16 July 2018  
© Springer Science+Business Media, LLC, part of Springer Nature 2018

## Abstract

Moisture sorption isotherms of chironji kernels were determined at 25, 35 and 45 °C over a water activity range of 0.11–0.93. Three sorption models i.e., Guggenheim–Anderson–de Boer (GAB), Brunauer–Emmett–Teller (BET) and Caurie were evaluated to find out their fitness to the sorption data. Thermodynamic properties of sorbed water were analyzed over the selected range of water activity and temperature. The result showed that the sorption isotherms reflected Type II BET sorption characteristics with a clear hysteresis at the temperatures. Of the three models, GAB and Caurie models were found superior predicting the sorption of chironji kernels over the entire range of water activity values. The monolayer moisture content values calculated by the best-fitted GAB and Caurie model for adsorption were 9.86 and 6.31%, 8.023 and 6.18%, 6.90 and 5.97% (db) and for desorption were 6.53 and 6.01%, 5.85 and 5.68%, 4.21 and 5.60% (db), respectively at 25, 35 and 45 °C. The value of isosteric heat decreased with increasing moisture content and approached the latent heat of pure water. Sorption entropy increased with increasing moisture content and decreased gradually with increase in moisture content. The spreading pressures, for both adsorption and desorption, increased with increasing water activity at the three selected temperatures.

**Keywords** Sorption isotherms · Hysteresis · Monolayer moisture content · Isosteric heat · Spreading pressure

## Introduction

Chironji (*Buchanania lanzan* Spreng.), a member of family Anacardiaceae, is an industrially important tree, distributed extensively throughout India, Burma, Bhutan, and Nepal. These naturally growing trees possess versatile properties and all most all parts of the tree are used in diverse ways to treat a variety of health issues [1]. Among seven wild species of *Buchanania* found in India, *B. lanzan* and *B. axillaries* yield edible fruit, tannin, and gum [2].

Chironji kernels are rich in fat, protein, and dietary fibres, and contain high calorific value—about 656 kcal per 100 g [2]. The kernels possesses various bioactive components which can be processed into high-value products such as functional foods, beverages, and nutritional supplements [3]. The chironji kernels are rich source of oleic acid, which plays an important role in activation of various pathways of the immune component cell and reduces the inflammatory effect of long chain fatty acid [4]. Chironji kernels possess anti-oxidant, anti-anaemic, anti-cough, anti-leprotic, anxiolytic, and anti-depressant properties [5–7]. The anti-inflammatory and antioxidant activity of chironji seeds revealed the presence of alkaloids, polyphenols, glycosides, phytosterols, sitosterol, and stigmasterol, which have substantial applications in food, nutraceutical and pharmaceutical industries [8]. Chironji kernels are extensively utilized for preparation of various snacks, sweets, beverages, additives and many health-promoting functional foods. Chironji kernels have excellent demand in international markets and thus, it has become one of the important industrial crops in the current scenario.

✉ J. K. Sahu  
jksahu@iitd.ac.in

<sup>1</sup> Food and Bioprocess Engineering Laboratory, Centre for Rural Development and Technology, Indian Institute of Technology Delhi, New Delhi 110016, India

<sup>2</sup> School of Life Sciences, Sambalpur University, Sambalpur, Odisha 768019, India

<sup>3</sup> School of Environmental Sciences, Sambalpur University, Sambalpur, Odisha 768019, India

Although, there are various water-based criteria for indication of the stability of food products, one of the most critical parameters is water activity, mostly in relation with predicting growth of microorganisms, maintaining chemical stability, minimizing non-enzymatic browning and auto-catalytic lipid oxidation reactions, prolonging the activity of enzymes and vitamins and optimizing physical properties of foods. Moisture sorption isotherm refers to the equilibrium correlation between water activity and moisture content of a product at a specific storage condition. Analysis of moisture sorption characteristics at various storage conditions is important for estimation of technological performance and quality of stored food products, especially in the quantitative approach to predict the shelf-life of stored food products [9–11].

Moisture sorption isotherms of different food stored products at various storage conditions have been extensively reviewed by [9, 12–14]. Different two and three-dimensional models have been evaluated to find their fitness to the sorption data, and various properties of the adsorbed and desorbed water have been comprehensively analysed for many dry fruits, seeds, and kernels [11, 15].

Chironji kernels contain about 5–6% moisture and are prone to development of molds, fungi and other spoilage microorganisms during storage. Although chironji kernels are used extensively in domestic and industrial markets, the literature on their moisture sorption characteristics under different storage temperatures and humidity conditions is scarce in order to design appropriate drying, packaging, storage and handling system. The aim of the paper is to analyze the moisture sorption characteristics and thermodynamic properties of sorbed water of chironji kernels at 25, 35 and 45 °C.

## Materials and methods

### Raw material collection and its proximate analysis

Fully matured chironji fruits were harvested in the month of April from Bargarh district in western Odisha, India and cleaned using a manually operated cleaning and washing device (CS—54, Jastin K Engineering Co., India). The cleaned fruits were soaked overnight in normal water to remove seed coats. The fruits were washed with running water and dried in a hot air assisted tray dryer (Jain Scientific, India) for about 26 h to achieve a moisture content of 11–12% (db). The dried fruits were decorticated using a decorticator (D01, IPE, India). From the proximate analysis, it was obtained that the chironji kernels contained 3.12% (*wb*) moisture, 12.25% (*wb*) carbohydrate, 30.45%

(*wb*) protein and 50.72% (*wb*) fat (for all analyses,  $n = 3$ ,  $SD = < 0.045\%$ ).

### Determination of equilibrium moisture content

The static gravimetric method based on the isopiestic transfer of water vapour was adopted to obtain moisture sorption properties of chironji kernels. The method has been well adopted by many authors to determine equilibrium moisture content of different food samples under various storage conditions [16–18].

An experimental set-up (Fig. 1) was developed to determine the equilibrium moisture content of chironji kernels. The set-up essentially consists of a double-walled rectangular chamber made up of stainless steel. The space between the outer and inner wall was filled with glass wools in order to provide sufficient insulation to the chamber. There were three perforated SS trays located inside the chamber and three digital weighing balances (Model: CY 513, ACZET, India) were placed on each tray. Nine glass desiccators containing Petri-plates, one each, were placed on the weighing balance (accuracy =  $\pm 0.001$  mg). Nine inorganic salt solutions with water activity values ranging from 0.11 to 0.93 were placed at the bottom of the desiccators to achieve the desired relative humidity. The Petri-plates containing samples, one each, were kept on perforated ceramic platforms located inside the desiccators. A partial vacuum of around 600 mmHg was maintained inside the desiccators to accelerate the sorption process [19]. The desired temperature was achieved by circulating hot air inside the chamber and maintained by a control panel. Nine pressure gauges were fitted to the glass desiccators to monitor the vacuum pressure during the sorption. The front door of the chamber was fitted with transparent glass sheet so that change in weight of the samples could be noted from the outside without disturbing the sorption conditions maintained inside the chamber.

In order to create a controlled humidity environment inside the desiccators, nine saturated solutions (Table 1) were prepared which provided a wide range of relative humidity at 25, 35 and 45 °C. The volume of the salt solution was maintained about  $\frac{1}{4}$  of the total volume of the total space for the desiccant. 6–7 g of the chironji kernel (about 100–110 nos.) was weighed in the individual Petri-plates and placed in the vacuum desiccators. The samples were left for approximately 19–21 days under partial vacuum at the three selected temperatures so that moisture content of the sample reaches to the equilibrium state which was measured by getting constant values ( $\pm 0.001$  g) of three consecutive weight readings.

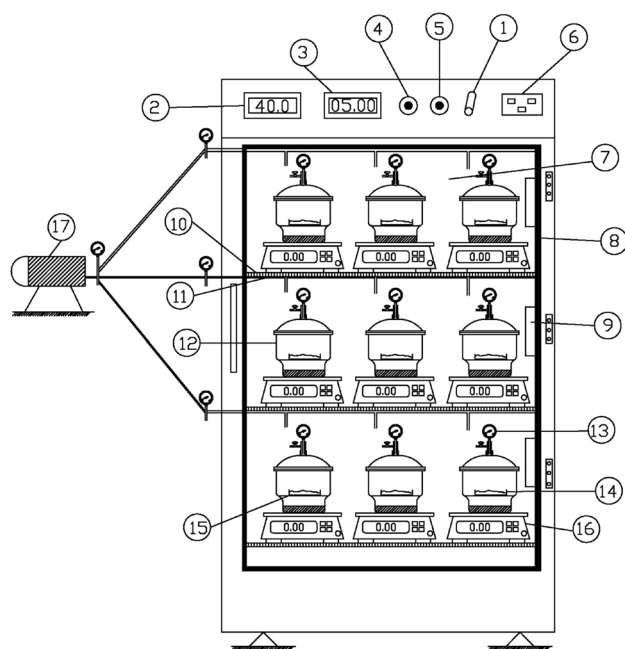


**Fig. 1** Schematic diagram of the experimental set-up used for determination of equilibrium moisture content of chironji kernels. 1 Power switch, 2 temperature display, 3 time display, 4 power display, 5 heating/cooling display, 6 control panel, 7 main chamber, 8 door gasket, 9 electrical panel, 10 perforated SS tray, 11 vacuum pipeline, 12 glass desiccator, 13 pressure gauge, 14 petri-plate, 15 perforated ceramic platform, 16 digital weighing balance, and 17 vacuum pump

**Table 1** Relative humidity of salt solution at 25, 35 and 45 °C [20, 21]

Salt solution	Temperature (°C)		
	25	35	45
Lithium chloride	11.30	11.25	11.16
Lithium iodide	17.56	15.57	13.49
Magnesium chloride	32.75	32.05	31.10
Potassium carbonate	43.16	43.20	43.10
Magnesium nitrate	52.89	49.91	46.83
Potassium iodide	68.86	66.96	65.26
Sodium nitrate	74.25	72.06	69.99
Ammonium sulphate	80.99	80.27	79.56
Potassium nitrate	93.58	90.79	87.03

## Modeling of sorption data

The moisture sorption data determined at 25, 35 and 45 °C were modeled into Guggenheim–Anderson–de Boer (GAB) [22], Brunauer–Emmett–Teller (BET) [23] and Caurie [24] models as these two and three dimensional models provide an estimation of the monolayer moisture content which describes the stable moisture content of a food product at a particular temperature and relative humidity.

### GAB model

$$\frac{M}{M_m} = \frac{C_g k a_w}{(1 - k a_w)(1 - k a_w - C_g k a_w)} \quad (1)$$

### BET model

$$\frac{M}{M_m} = \frac{C_b a_w}{(1 - a_w)(1 - a_w - C_b a_w)} \quad (2)$$

### Caurie model

$$M = \exp \left[ a_w \times \ln(C_c) - \frac{1}{4.5 \times M_m} \right] \quad (3)$$

where,  $a_w$  is the water activity (decimal),  $M$  is the equilibrium moisture content (kg per kg dry solid),  $M_m$  is the monolayer moisture content (kg per kg dry solid),  $C_g$  is GAB constant,  $k$  is GAB constant associated with multi-layer molecules,  $C_b$  and  $C_c$  are the BET and Caurie's constant, respectively.

Temperature dependency of GAB model constants  $C_g$  and  $k$  was expressed by the given Arrhenius-type equation [13].

$$c = c_o \exp \left[ \frac{\Delta H_c}{RT} \right] = c_o \exp \left[ \frac{Q_m - Q_n}{RT} \right] \quad (4)$$

$$k = k_o \exp \left[ \frac{\Delta H_k}{RT} \right] = k_o \exp \left[ \frac{Q_c - Q_n}{RT} \right] \quad (5)$$

where,  $\Delta H_c$  is the net heat ( $\text{kJ mol}^{-1}$ ) between monolayer and multilayer sorption,  $\Delta H_k$  is the net heat ( $\text{kJ mol}^{-1}$ ) between the heat of condensation of pure water and multilayer sorption,  $Q_m$  is the total heat ( $\text{kJ mol}^{-1}$ ) of sorption of monolayer,  $Q_n$  is the total heat ( $\text{kJ mol}^{-1}$ ) of sorption of multilayer covering monolayer,  $Q_c$  is the heat of condensation of pure water ( $43.53 \text{ kJ mol}^{-1}$  at 35 °C i.e., mean temperature),  $c_o$  and  $k_o$  are constants of entropic character,  $R$  is the ideal gas constant ( $8.314 \text{ kJ mol}^{-1} \text{ K}^{-1}$ ), and  $T$  is the storage temperature ( $K$ ). A nonlinear regression analysis of the GAB model was adopted to calculate the values of  $c_o$ ,  $k_o$ ,  $M_m$ ,  $Q_m$  and  $Q_n$  combining Eqs. (1), (4) and (5). A MATLAB (R2017a) program was prepared using nonlinear regression analysis to calculate the coefficients and to evaluate the fitness of sorption data to the selected models. While evaluating the fitness of the BET model to the actual sorption data, water activity values up to 0.4 were considered as BET model is valid up to  $a_w = 0.4$  [25]. The fitness of models was estimated by computing the values of coefficient of determination ( $R^2$ ), relative deviation percent ( $R_d$ ), average residuals ( $e_{avg}$ ) and root mean square error ( $R_{MSE}$ ) between the actual and predicted values of emc. The values of these statistical parameters were computed by using Eqs. (6) to (9), respectively.

$$R^2 = 1 - \frac{\sum_{i=1}^N (M_{ei} - M_{pi})^2}{\sum_{i=1}^N (M_{ei} - \sum_i \frac{M_{ei}}{N})^2} \quad (6)$$

$$R_{dev} = \frac{100}{N} \sum_{i=1}^N \left| \frac{M_{ei} - M_{pi}}{X_{ei}} \right| \quad (7)$$

$$e_{avg} = \sum_{i=1}^N \left( \frac{M_{ei} - M_{pi}}{N} \right) \quad (8)$$

$$R_{MSE} = \left[ \frac{1}{N} \sum_{i=1}^N (M_{ei} - M_{pi}) \right]^{0.5} \quad (9)$$

where,  $M_{ei}$  and  $M_{pi}$  are actual and predicted emc values respectively, and  $N$  is the number of observations. When the values of  $R_d$  and  $e_{avg}$  are less than 10%, the goodness of fit describes its acceptability [26].

### Determination of thermodynamic properties of sorbed water

#### Determination of sorbed surface area

The thermodynamic properties of chironji kernels were calculated at the mean temperature of the study. The sorbed surface area  $A_s$  ( $\text{m}^2 \text{g solid}^{-1}$ ) of chironji kernels was calculated by using following equation [27].

$$A_s = \frac{100 \times M_m N_A A_w}{M_w} = 3530 \times M_m \quad (10)$$

where,  $M_m$  is the BET monolayer moisture content (kg per kg dry solid),  $M_w$  is the molecular weight of water molecule ( $18 \text{ kg kmol}^{-1}$ ),  $N_A$  is the Avogadro's number ( $6 \times 10^{26} \text{ molecules kmol}^{-1}$ ), and  $A_w$  is the surface area of a sorbed water ( $1.06 \times 10^{-19} \text{ m}^2$ ).

#### Determination of heat of sorption

The moisture sorption data predicted by the best-fitted sorption model at the three selected temperatures was used to calculate the isosteric heat of sorption by linearization of the Clausius–Clapeyron equation as below [28].

$$q_{st} = -R \left[ \frac{d[\ln a_w]}{d\left(\frac{1}{T}\right)} \right]_M \quad (11)$$

where,  $a_{w1}$  and  $a_{w2}$  are the values of water activity (decimal) at two temperatures  $T_1$  and  $T_2$  (K) respectively,  $q_{st}$  is the isosteric heat of sorption, and  $R$  is the ideal gas constant. By assuming a specific moisture content  $M$ , the value water activity  $a_w$  was predicted by using the best-fitting sorption model. A linear graph between  $\ln a_w$  and  $1/T$  was plotted and the value of  $q_{st}$  was calculated from the slope of the graph. In the calculation, the value of  $M$  is assumed up to monolayer value  $M_m$  as obtained by the best-fitted sorption model. By using the Excel spreadsheet in MS office 2013, the calculation of  $a_w$  values analogous to a specific moisture content  $M$  was achieved.

The value of the isosteric heat of sorption,  $Q_{st}$  was determined from the following relationship.

$$Q_{st} = q_{st} + Q_c \quad (12)$$

where,  $Q_c$  is the heat of condensation of pure water ( $43.53 \text{ kJ mol}^{-1}$ ) at the mean temperature ( $35 \text{ }^\circ\text{C}$ ) used in this study.

#### Determination of sorption entropy

The sorption entropy was calculated by fitting Eq. (13) to the sorption data predicted by the best-fitting sorption model as below [29].

$$-\ln a_w = \frac{Q_{st}}{RT} - \frac{\Delta S}{R} \quad (13)$$

where,  $\Delta S$  is the entropy ( $\text{kJ mol}^{-1}$ ). The value  $\Delta S$  was computed from the intercept ( $\Delta S/R$ ) value of the plot between  $\ln a_w$  and  $1/T$  for definite values of moisture content.

#### Determination of spreading pressure

Spreading pressure, known as surface potential, represents the surface excess free energy. It acts as a second pressure and results in an increase in surface tension on bare sorption locations due to the sorbed molecules on them. The spreading pressure was calculated using Eq. (14) [30].

$$\phi = \frac{K_B T}{A_w} \ln \left[ \frac{1 + b_0 a_w - b a_w}{1 - b a_w} \right] \quad (14)$$

where,  $K_B$  is the Boltzmann's constant ( $1.38 \times 10^{-23} \text{ JK}^{-1}$ ),  $T$  is the temperature (K) and  $A_w$  is the surface area of a water molecule ( $1.06 \times 10^{-19} \text{ m}^2$ ),  $b_0$  and  $b$  are dimensionless constants. In order to calculate the values of  $b$  and  $b_0$ , Dent sorption model (Eq. 15) was used [31].

$$\frac{a_w}{M} = \frac{1}{b_0 M_m} + \frac{b_0 - 2b}{b_0 M_m} + \frac{b(b_0 - b)}{b_0 M_m} a_w^2 \quad (15)$$

where,  $a_w$  is the water activity (fraction),  $M$  is the equilibrium moisture content (kg per kg dry solid) and  $M_m$  is the

monolayer moisture content (kg per kg dry solid). By non-linear regression analysis of the actual data and using  $M_m$  values predicted by the BET model, the values of  $b$  and  $b_0$  were obtained.

## Results and discussion

### Sorption isotherms of chironji kernels

Figure 2 presents the variation of emc values with equilibrium relative humidity at the three temperatures. From the figure, it is apparent that both adsorption and desorption

isotherms exhibit a concurrent increase in the emc values with increasing values of Rh. In the first section (with low Rh) of the sorption plots, the sorbed chironji kernels were having relatively lower amount of moisture. Conversely, a large portion of moisture was absorbed in higher Rh values. This trend is manifested in the form of the sigmoid-shaped curve; describing Type II moisture sorption characteristics [32]. Similar results were reported for many dry fruits such as walnut kernels [33], melon seeds [34], and cowpeas [35].

It is also apparent from Fig. 2 that the sorption isotherms of chironji kernels exhibited hysteresis effect over the entire range of water activity at the three temperatures. The degree of hysteresis increased with increasing values of water

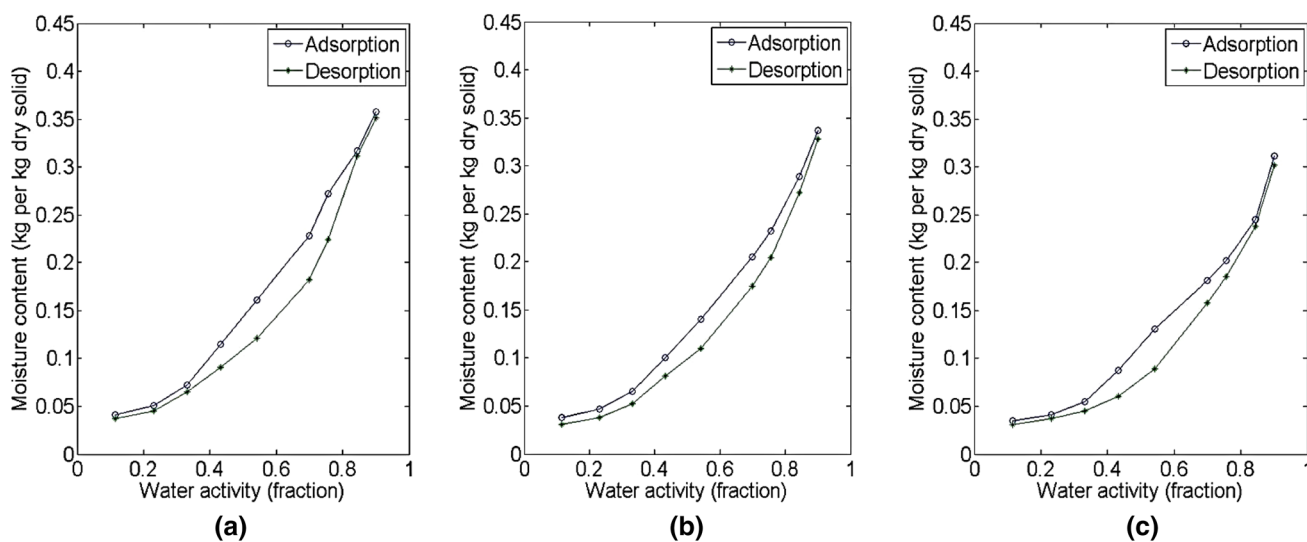
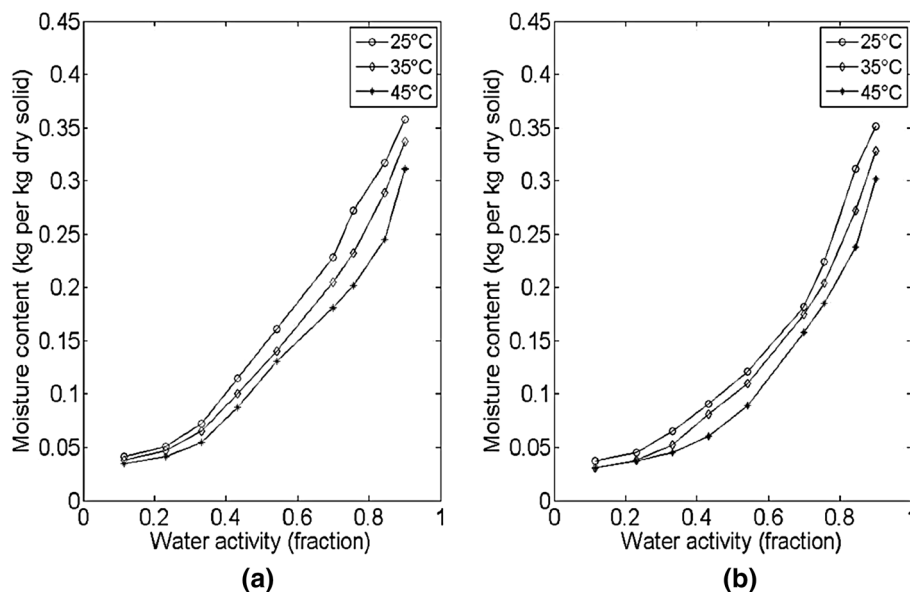


**Fig. 2** Adsorption and desorption isotherms of chironji kernels at **a** 25 °C, **b** 35 °C and **c** 45 °C

**Fig. 3** Effect of temperatures on **a** adsorption and **b** desorption isotherms of chironji kernels at 25, 35 and 45 °C



activity, became pronounced, and diminished gradually at high water activity ranges. Such kind of hysteresis effect was also reported for black gram [16], walnut kernels [33], apricot and cowpea [35], cashew nuts [36], almond [37] and hazelnut [38]. Since food is a complex biological material consisting of various macro- and micro-elements, there is no sufficient justification to explain hysteresis effect in a food sample [9].

Figure 3 shows the behaviour of the moisture sorption isotherms of chironji kernels with various temperatures. The figures showed that at a particular relative humidity, the emc values declined with an increase in temperature, thus signifying that chironji kernels became less hygroscopic at higher storage temperatures. Since the chironji kernels are rich in fat, this trend may be because of a decrease in available

**Table 2** Computed values of models constants fitted to the sorption data of chironji kernels

Sorption model	Constants	Adsorption			Desorption		
		25 °C	35 °C	45 °C	25 °C	35 °C	45 °C
GAB	$M_m$	0.098	0.080	0.069	0.065	0.058	0.042
	$C_g$	3.922	4.662	4.849	6.148	5.137	9.068
	$k$	0.861	0.888	0.896	0.939	0.948	0.993
	$R^2$	0.985	0.974	0.973	0.967	0.951	0.977
	$R_{dev}$	11.71	10.56	12.20	8.64	10.96	13.09
	$e_{ave}$	-0.0014	-0.0018	-0.0014	-0.0027	-0.0036	-0.0062
BET	$R_{MSE}$	0.0216	0.0178	0.0159	0.0209	0.0216	0.0323
	$M_m$	0.084	0.067	0.064	0.055	0.045	0.084
	$C_b$	3.716	4.233	5.896	5.411	7.728	3.716
	$R^2$	0.902	0.904	0.891	0.917	0.901	0.914
	$R_{dev}$	36.882	38.024	34.323	18.872	16.812	14.398
	$e_{ave}$	0.0997	0.0926	0.0698	0.0455	0.0321	0.0183
Caurie	$R_{MSE}$	0.2204	0.2007	0.1534	0.1097	0.0841	0.1039
	$M_m$	0.063	0.062	0.060	0.060	0.057	0.056
	$C_c$	17.839	17.322	17.252	18.905	21.953	20.163
	$R^2$	0.992	0.991	0.994	0.993	0.994	0.997
	$R_{dev}$	7.347	7.311	8.031	3.626	4.16	5.407
	$e_{ave}$	0.0014	0.0011	0.0005	-0.0006	-0.0005	-0.0014
	$R_{MSE}$	0.0167	0.0130	0.0109	0.0070	0.0036	0.0073

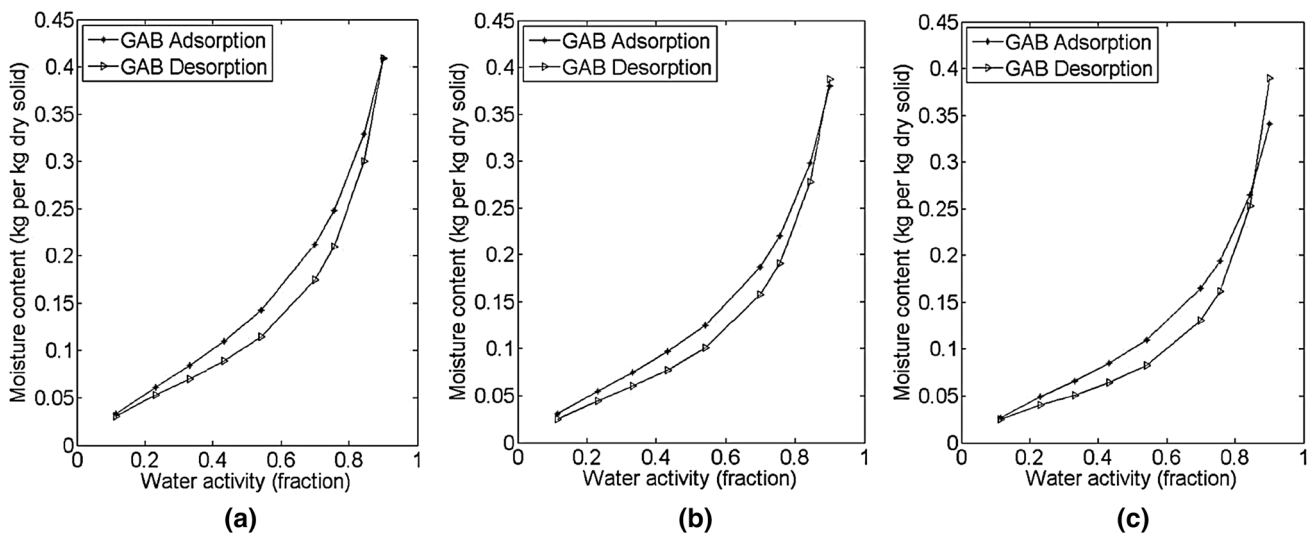
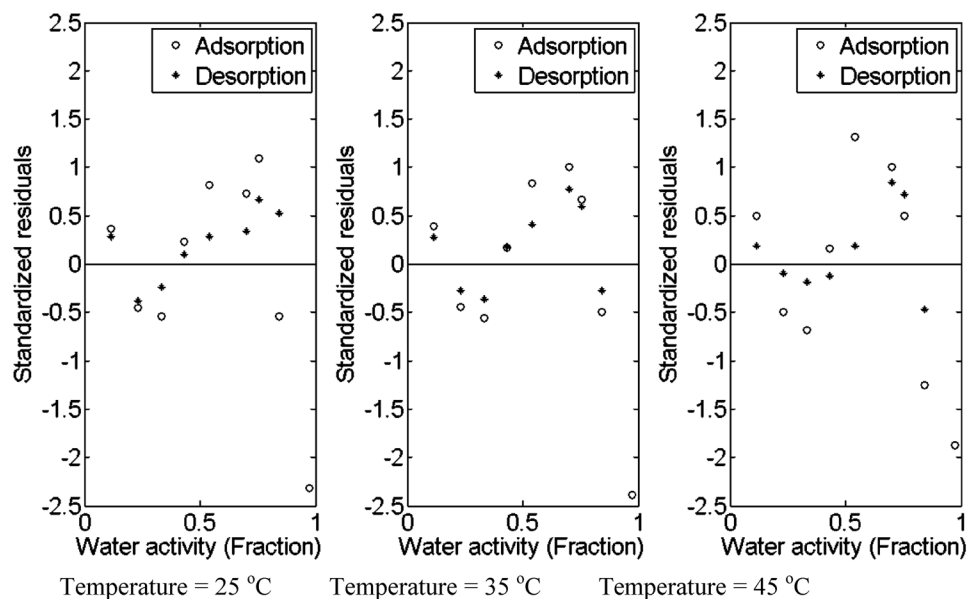
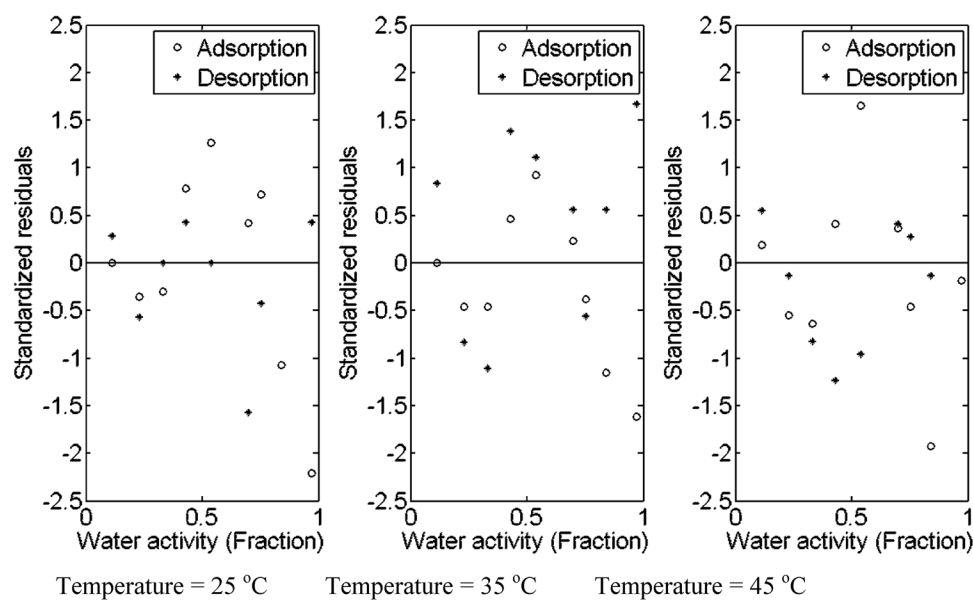


**Fig. 4** Adsorption and desorption isotherms of chironji kernels predicted by the best-fitted GAB model at **a** 25 °C, **b** 35 °C and **c** 45 °C

**Fig. 5** Standardized residuals fit of **a** GAB and **b** Caurie model to sorption data of chironji kernels at *i* 25 °C, *ii* 35 °C and *iii* 45 °C



**(a)** GAB model



**(b)** Caurie model

active sites for binding water molecules due to higher temperatures [39].

### Fitting of moisture sorption models

Table 2 presents the values of model constants along with their  $R^2$ ,  $R_{dev}$ ,  $e_{avg}$ , and  $R_{MSE}$  values. Out of three models, GAB and Caurie models were found superior in predicting the adsorption and desorption data over the entire range

of water activity and temperature values as exhibited by higher values of  $R^2$ , and lower values of  $R_{dev}$ ,  $e_{avg}$ , and  $R_{MSE}$ . The values of  $R^2$ ,  $R_{dev}$ ,  $e_{avg}$ , and  $R_{MSE}$  ranged from 0.951 to 0.985, 8.64 to 13.09,  $-0.001$  to  $-0.006$ , and  $-0.005$  to 0.001, respectively, for GAB model, whereas the values varied from 0.991 to 0.997, 3.62 to 8.03,  $-0.005$  to 0.001, and 0.003 to 0.016, respectively for Caurie model. The adsorption and desorption isotherms of chironji kernels predicted by the best-fitted GAB model is shown in

Fig. 4. It is also observed from Table 2 that the values  $M_m$ , estimated for the three models, decreased concurrently with increasing temperature from 25 to 45 °C for both the adsorption and desorption process. The ANOVA showed that adsorption and desorption data at the three selected temperatures were significantly different at  $P > 0.05$ . The  $M_m$  values calculated by the best-fitted GAB and Caurie model for adsorption were 9.86 and 6.31%, 8.023 and 6.18%, 6.90 and 5.97% (db) at 25, 35, and 45 °C, respectively. Similarly, the  $M_m$  value for desorption were 6.53 and 6.01%, 5.85 and 5.68%, 4.21 and 5.60% (db) at the respective temperatures. The values of GAB and Caurie model constants increased constantly with an increase in temperature during adsorption; however, there was no specific trend observed during desorption. The result has a good agreement with the findings reported by Vega-Gálvez et al. [40] and Togrul and Arslan [33].

Effect of temperature on GAB model constants was evaluated using Eqs. (4) and (5). The values of  $\Delta H_c$  and  $\Delta H_k$  were calculated to be  $-8.4$  and  $-1.59$  kJ mol $^{-1}$ ; and  $-14.98$  and  $-2.17$  kJ mol $^{-1}$  for adsorption and desorption, respectively, with values of  $R^2 = 0.915$  and  $R^2 = 0.956$ , respectively. The  $\Delta H_c$  value for adsorption is lower than the value for desorption. The negative  $\Delta H_c$  values indicate weaker bonds between solids and monolayer water molecules than between monolayer and multilayer water molecules inferring endothermic interaction of water molecules with the sample matrix [41]. A similar finding has been reported by Myhara et al. [42] while studying adsorption isotherms of Khalas dates. The negative  $\Delta H_k$  values indicate that there is an exothermic interaction of water molecules with the sorption locations of the sample structure. A negative  $\Delta H_k$  value is usually expected due to the weaker bonding of multilayer molecules in a sample matrix [11, 43].

The fitness of the GAB and Caurie models to the actual sorption data was further analyzed by calculating the standardized residuals as defined below.

$$r = \frac{(e_i - e_{avg})}{R_{MSE}} \quad (16)$$

where,  $e_i$  is the difference between the actual and predicted values of emc. The standardized residual plots of GAB and Caurie model at the three selected temperatures are shown in Fig. 5. The residual plots for both GAB and Caurie model displayed uniformly distributed pattern at the three temperatures indicating that the models are best fitted to the actual sorption data.

## Thermodynamic properties of the sorbed water

### Sorbed surface area

The values of surface area  $A_s$  as calculated using Eq. (7) by substituting the values of  $M_m$  (Table 2) obtained by BET model were 321.803 and 225.620, 295.122 and 194.397, and 243.024 and 159.091 m $^2$ g solids $^{-1}$  for adsorption and desorption, respectively, at 25, 35, and 45 °C. The value of  $M_m$  in the BET model is an indication of sorption ability of the sorbent and shows the effectiveness of active sites for water vapor [44].

### Heat of sorption

Figure 6 shows the variation in the isosteric heat of sorption with the moisture content of chironji kernels. The value of  $q_{st}$  for both adsorption and desorption increased to a maximum and then declined gradually with increase in values of  $M$ . The maximum value of  $q_{st}$  for adsorption was 10.44 kJ mol $^{-1}$  at  $M = 7.5\%$  (db), where the value was 15.53 kJ mol $^{-1}$  for desorption at  $M = 5\%$  (db). The positive values imply an endothermic reaction due to the extraction

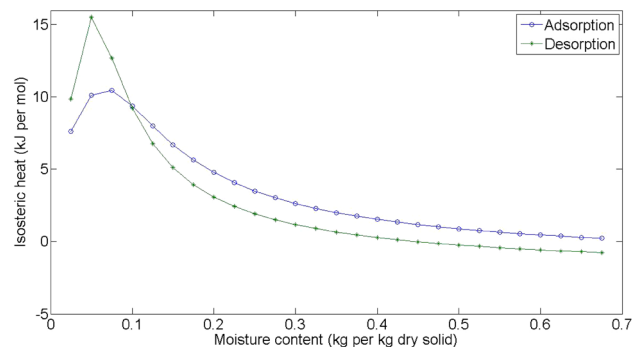


Fig. 6 Variation of isosteric heat of sorption with moisture content of chironji kernels

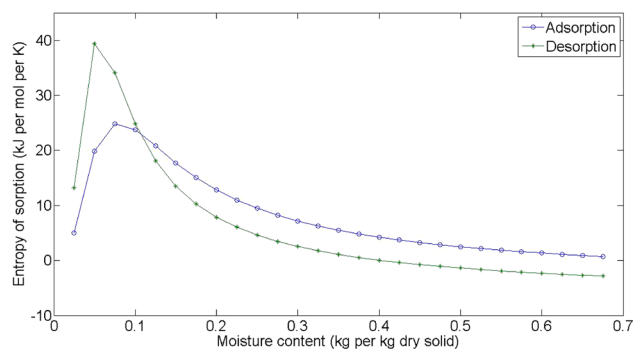


Fig. 7 Variation of sorption entropy with moisture content of chironji kernels



**Table 3** Spreading pressure of chironji kernels at 25, 35 and 45 °C

Water activity	Spreading pressure (J m <sup>-2</sup> )					
	Adsorption			Desorption		
	25 °C	35 °C	45 °C	25 °C	35 °C	45 °C
0.114	0.0150	0.0157	0.0180	0.0219	0.0212	0.0286
0.231	0.0288	0.0301	0.0340	0.0395	0.0387	0.0497
0.331	0.0401	0.0418	0.0468	0.0530	0.0522	0.0651
0.432	0.0516	0.0538	0.0596	0.0660	0.0655	0.0798
0.541	0.0648	0.0675	0.0741	0.0804	0.0801	0.0958
0.699	0.0873	0.0908	0.0986	0.1043	0.1046	0.1218
0.755	0.0973	0.1011	0.1094	0.1146	0.1152	0.1330
0.843	0.1174	0.1220	0.1311	0.1352	0.1365	0.1552
0.934	0.1367	0.1419	0.1518	0.1548	0.1566	0.1762

of sugars in the solution. As a consequence, the value of  $Q_{st}$  was smaller than the value of  $Q_c$ . The values of  $q_{st}$  for adsorption is lower than those for desorption, which means that during the desorption process there are more polar locations on the surface of the chironji kernels and the energy of binding is higher [45]. Similar results are reported for melon seeds [34], and pistachio nuts [46]. The physical explanation for the steep increase of  $q_{st}$  at low moisture contents is that, in the initial stage of sorption, there are highly active polar locations on the surface of the chironji kernels which are covered with water molecules forming a monomolecular layer. The value of  $q_{st}$ , which is significantly lower than  $\Delta H_{vap}$ , suggests physical sorption of the water on the polar groups of the biopolymer with hydrogen bonds and with Van der Waals' forces [47, 48]. For a moisture content of less than 10%, there is no dissolution or plasticization of the biopolymer [47]. For higher moisture content, the  $q_{st}$  is higher than  $\Delta H_{vap}$  which means that the second layer of water molecules is formed at the surface of the multilayer sorption while the binding energy between water molecules and the sorption sites is higher than the energy of pure water molecules [49]. Dissolution of sugars and macromolecular biopolymers, as well as capillary condensation effects, become the predominant actions in higher moisture range. The value of  $q_{st}$  tends to zero and the corresponding moisture content (for  $q_{st} = 0$ ) can be considered as the limit of bound water [11].

### Sorption entropy

Variation of sorption entropy with moisture content is shown in Fig. 7. The figure shows that the values of adsorption entropy increased rapidly with increasing moisture content; the maximum value obtained was 24.79 kJ mol<sup>-1</sup> at 7.5% (db). The value decreased abruptly with an increase in moisture content and subsequently, attained a constant value. A similar trend was observed for desorption entropy where

the value increased smoothly with an increase in moisture content to a value of 39.42 at 5% (db). The value declined gradually with increasing moisture content.

### Spreading pressure

The values of spreading pressures ( $\phi$ ) as computed using Eq. (16) are presented in Table 3. The table shows that for both adsorption and desorption, the value of  $\phi$  increased (0.0150–0.1518 J m<sup>-2</sup> for adsorption and 0.0212–0.1762 J m<sup>-2</sup> for desorption) over the entire range of water activity and temperature. The value of  $\phi$  for adsorption increased with increasing temperatures at all water activity values; however, no particular trend was observed for desorption. This type of trend has been reported by Zhang et al. [50] and Torres et al. [51] while studying the moisture sorption characteristics of glutinous rice flour and different plant-based gums, respectively.

### Conclusions

The sorption isotherms of chironji kernels had a sigmoid profile at 25, 35 and 45 °C. The equilibrium moisture contents were found to decline with increasing temperature at particular water activity. The trend also suggests that at a particular temperature, the emc increases with increasing water activity. Hysteresis was reasonable over the complete variety of water activity. GAB and Caurie models were found the most suitable for predicting the sorption data accurately over the entire range of water activity and temperature range. The analysis presented in this work would provide a fundamental baseline to formulate the safe storage guidelines for chironji kernels.

**Acknowledgements** Financial support from the Ministry of Sciences and Technology, Govt. of India is highly acknowledged. Grant No. SP/YO/070/2017(G).

## Compliance with ethical standards

**Conflict of interest** The authors declare that they have no competing interests.

## References

1. S.K. Malik, R. Chaudhury, O.P. Dhariwal, D.C. Bhandari, *Genetic Resources of Tropical Underutilized Fruits in India*, 1st edn. (National Bureau Of Plant Genetic Resources, New Delhi 2010)
2. The Wealth of India. (C.S.I.R. New Delhi, 1988), <http://www.niscair.res.in/ActivitiesandServices/Products/Woi1.htm>, Accessed 12 Apr 2018
3. N. Khatoon, R.K. Gupta, Y.K. Tyagi, J. Pharm. Phytochem. **4**, 87–94 (2015)
4. S.N. Sahu, S.G. Jaiswal, S.N. Naik, J. Lipid Sci. Technol. **47**, 1–3 (2015)
5. J. Ankur, S. Priyanka, N. Vyas, J. Khan, S. Malviya, A. Kharia, Eur. J. Biomed. Pharm. Sci. **4**, 800–803 (2017)
6. M. Gupta, B. Shaw, Ind. J. Tradit. Knowl. **8**, 372–378 (2009)
7. M.K. Singh, B.K. Das, P. Patidar, Ind. J. Pharm. **48**, 214–215 (2016)
8. A. Warokar, M. Ghante, N. Duragkar, K. Bhusari, Ind. J. Pharm. Ed. Res. **44**, 363–368 (2010)
9. H.A. Iglesias, J. Chirife, *Handbook of Food Isotherms: Water Sorption Parameters for Food and Food Components* (Academic Press, New York, 1982), pp. 673–675
10. K.A. Nelson, T.P. Labuza, J. Food Eng. **22**, 271–289 (1994)
11. E. Tsami, Z.B. Maroulis, D. Marinos-Kouris, G.D. Saravacos, Int. J. Food Sci. Technol. **25**, 350–359 (2007)
12. A.H. Al-Muhtaseb, W.A.M. McMinn, T.R.A. Magee, Food Bioprod. Proc. **80**, 118–128 (2002)
13. S. Basu, U.S. Shivhare, A.S. Mujumdar, Dry Technol. **24**, 917–930 (2006)
14. L.N. Bell, T.P. Labuza, Am. Assoc. Cereal. Chem. **2**, 33–36 (2000)
15. E. Ayranci, G. Ayrance, Z. Dogantan, J. Food. Sci. **55**, 1591–1593 (1990)
16. S.S. Baslingappa, S.K. Das, B. Maiti, J. Food Eng. **67**, 477–482 (2005)
17. R.A. Calzetta, R.J. Aguerre, C. Suárez, J. Food Eng. **42**, 51–57 (1999)
18. D. Choudhury, J.K. Sahu, G.D. Sharma, Ind. Crops Prod. **33**, 211–216 (2011)
19. R. Moreyra, M. Paleg, J. Food Eng. **46**, 1918 (1981)
20. C. Arai, S. Hosaka, K. Murase, Y. Sano, J. Chem. Eng. Jpn. **9**, 328–330 (1976)
21. L. Greenspan, J. Res. Natl. Bur. Stan. **81**, 89–96 (1976)
22. C. van Den Berg, S. Bruin. *Water Activity: Influences on Food Quality*, ed. by L.B. Rockland, G.F. Stewart (Academic Press, New York, 1981), pp. 2–61
23. J. Chirife, H.A. Iglesias, Int. J. Food Sci. Technol. **13**, 159–174 (1978)
24. M. Laurie, in *Water Activity: Influences on Food Quality*, ed. by L.B. Rockland, G.F. Stewart (Elsevier, New York, 1981), pp. 63–87
25. T. Labuza, Food Technol. **22**, 263–272 (1968)
26. H. Das, *Food Processing Operations Analysis*, 1st edn. (Asian Books Pvt. Ltd, New Delhi, 2005), pp. 362–363
27. S.J. Gregg, J. Sidney, K.S.W. Sing, *Adsorption, Surface Area, and Porosity*, 2nd edn. (Academic Press, New York, 1982)
28. E. Tsami, M.K. Krokida, A.E. Drouzas, J. Food Eng. **38**, 381–392 (1999)
29. R.J. Aguerre, C. Suarez, P.E. Viollaz, J. Food Sci. **51**, 1547–1549 (1986)
30. O.O. Fasina, O.O. Ajibola, R.T. Tyler, J. Food Proc. Eng. **22**, 405–418 (1999)
31. R.W. Dent, Text. Res. J. **47**, 145–152 (1977)
32. S. Brunauer, L.S. Deming, W.E. Deming, E. Teller, J. Am. Chem. Soc. **62**, 1723–1732 (1940)
33. H. Toğrul, N. Arslan, J. Stored Prod. Res. **43**, 252–264 (2007)
34. N. Aviara, O. Ajibola, J. Food Eng. **55**, 107–113 (2002)
35. E. Ayranci, O. Duman, J. Food Eng. **70**, 83–91 (2005)
36. K.O. Falade, J.J. Chime, O.S. Ogunwolu, Agric. Environ. **22**, 83–87 (2004)
37. L.Z. Taitano, R.P. Singh, J.H. Lee, F. Kong, J. Food Process Eng. **35**, 840–850 (2012)
38. D. Güzey, M. Özdemir, F.G. Seyhan, H. Doğan, Y.O. Devres, Dry Technol. **19**, 691–699 (2001)
39. G. Mazza, M. Lemaguer, Int. J. Food Sci. Technol. **15**, 181–194 (2007)
40. A. Vega-Gálvez, M. Palacios, R. Lemus-Mondaca, C. Passaro, Quím. Nova **31**, 1417–1421 (2008)
41. M. Sormoli, T. Langrish, Food Sci. Technol. **62**, 875–882 (2015)
42. R.M. Myhara, M.S. Taylor, B.A. Slominski, I. Al-Bulushi, J. Food Eng. **37**, 471–479 (1998)
43. A.L. Gabas, F.C. Menegalli, J. Telis-Romero, J. Food Sci. **65**, 680–680 (2000)
44. D.S. Chung, H.B. Pfost, Trans. ASAE **10**, 552–555 (1967)
45. A.L. Benado, S.S.H. Rizvi, J. Food Sci. **50**, 101–105 (1985)
46. M.A.M. McMinn, A.H. Al-Muhtaseb, T.R.A. Magee, J. Food Proc. Eng. **26**, 323–338 (2003)
47. G.N. Roman, M.J. Urbicain, E. Rotstein, J. Food Sci. **47**, 1484–1488 (1982)
48. C. Van Oss, R. Good, R.M. Chaudhury, J. Colloid Interface Sci. **111**, 378–390 (1986)
49. M. Masuzawa, C. Sterling, Biopolymers **6**, 1453–1459 (1968)
50. H. Zhang, Y. Bai, X. Zhao, R. Duan, Am. J. Food Technol. **11**, 115–124 (2016)
51. M.D. Torres, R. Moreira, F. Chenlo, M.J. Vázquez, Carbohydr. Polym. **89**, 592–598 (2012)